Diagnostics of polarization purity of x rays by means of Rayleigh scattering

A. Surzhykov,[1,2] V. A. Yerokhin,[1,3] S. Fritzsche,[4,5] and A. V. Volotka[4,6]
[1]Physikalisch-Technische Bundesanstalt, D-38116 Braunschweig, Germany
[2]Technische Universität Braunschweig, D-38106 Braunschweig, Germany
[3]Center for Advanced Studies, Peter the Great St. Petersburg Polytechnic University, 195251 St. Petersburg, Russia
[4]Helmholtz-Institut Jena, D-07743 Jena, Germany
[5]Theoretisch-Physikalisches Institut, Friedrich-Schiller-Universität Jena, D-07743 Jena, Germany
[6]Department of Physics, St. Petersburg State University, 198504 St. Petersburg, Russia

(Received 12 September 2018; published 6 November 2018)

Synchrotron radiation is commonly known to be completely linearly polarized when observed in the orbital plane of the synchrotron motion. Under actual experimental conditions, however, the degree of polarization of the synchrotron radiation may be lower than the ideal 100%. We demonstrate that even tiny impurities of polarization of the incident radiation can drastically affect the polarization of the elastically scattered light. We propose to use this effect as a precision tool for the diagnostics of the polarization purity of the synchrotron radiation. Two variants of the diagnostics method are proposed. The first one is based on the polarization measurements of the scattered radiation and relies on theoretical calculations of the transition amplitudes. The second one involves simultaneous measurements of the polarization and the cross sections of the scattered radiation and is independent of theoretical amplitudes.

DOI: 10.1103/PhysRevA.98.053403

I. INTRODUCTION

Advent of third-generation synchrotron radiation facilities made possible scattering experiments of a novel type, where the linear polarizations of both the incident and the scattered particles (photons and/or electrons) were detected [1–4]. These experiments measured polarization correlations and the polarization transfer between the incident and scattered beams. They demonstrated that the detection of polarization properties of the scattered particles could be used for an accurate determination of the polarization properties of the incident beam.

In the present work, we consider the elastic (Rayleigh) scattering of the synchrotron radiation off a closed-shell atomic target. The synchrotron radiation is known to be 100% linearly polarized when observed in the orbital plane of the synchrotron motion. It is also well-known that the elastic scattering of a fully linearly polarized x-rays on a closed-shell atomic target preserves the polarization and thus yields a fully linearly polarized scattered radiation. This is an exact statement that follows from the symmetry requirements [5]. As a consequence, one might expect a fully linearly polarized scattered radiation as an outcome of the process.

A closer examination, however, shows that this is not always the case. In particular, a recent experiment [6] found a strong depolarization of the synchrotron radiation scattered off the gold target, with the degree of polarization of $27 \pm 12\%$ if observed at the angle $\theta = 90^\circ$. The explanation of this phenomenon is twofold: first, in practice, the synchrotron radiation turns out to be slightly depolarized (in the case of Ref. [6], by about 2%) and, second, the small depolarization of the initial radiation has a drastically amplified effect on the polarization of the scattered radiation.

In this work, we present a detailed investigation of the effect of strong depolarization of the elastically scattered light. We demonstrate that this effect can be used as a precision tool for the diagnostics of the polarization purity of the x-ray radiation. The proposed method can detect very small deviations of the degree of the linear polarization from 100%, which is beyond detection possibilities of other methods such as the traditional Compton polarimetry.

The proposed detection technique can become an important tool in investigations of various effects that use the synchrotron radiation and strongly depend on purity of its polarization, such as studies of the x-ray magnetic linear or circular dichroism [7,8], the x-ray magnetic scattering [9], nuclear scattering [10], etc.

II. BASIC THEORY

We consider the process of the Raleigh scattering, namely, the elastic scattering of a photon on bound atomic electrons. Initially, we have an incoming photon with the momentum $\boldsymbol{k}_i$ and polarization $\boldsymbol{\epsilon}_i$, and an atomic state $|i\rangle$ with the energy E_i, the total angular momentum J_i, and its projection M_i. After the scattering, we have the scattered photon with the momentum $\boldsymbol{k}_f$ ($|\boldsymbol{k}_f| = |\boldsymbol{k}_i| = \omega$) and polarization $\boldsymbol{\epsilon}_f$, and an atomic state $|f\rangle$ with the energy $E_f = E_i$, the total angular momentum $J_f = J_i$, and its projection M_f. The amplitude of the process is given by [11]

$$\mathcal{M}_{fi} = -r_0 mc^2 \sum_\nu \left[\frac{\langle f|\hat{\mathcal{R}}^\dagger(\boldsymbol{k}_f, \boldsymbol{\epsilon}_f)|\nu\rangle \, \langle \nu|\hat{\mathcal{R}}(\boldsymbol{k}_i, \boldsymbol{\epsilon}_i)|i\rangle}{E_i - E_\nu + \omega + i0} + \frac{\langle f|\hat{\mathcal{R}}(\boldsymbol{k}_i, \boldsymbol{\epsilon}_i)|\nu\rangle \, \langle \nu|\hat{\mathcal{R}}^\dagger(\boldsymbol{k}_f, \boldsymbol{\epsilon}_f)|i\rangle}{E_i - E_\nu - \omega - i0} \right], \quad (1)$$

where $r_0 = e^2mc^2$ is the classical electron radius, the summation over ν goes over all possible intermediate electronic states of the atom, and $\hat{\mathcal{R}}(\hat{\mathcal{R}}^\dagger)$ is the operator of the absorbtion (emission) of a photon in the Coulomb (velocity) gauge,

$$\hat{\mathcal{R}} = \sum_m \boldsymbol{\epsilon} \cdot \boldsymbol{\alpha}_m \, e^{i\boldsymbol{k}\cdot\boldsymbol{r}_m} . \tag{2}$$

Here, m numerates electrons in the atom, $\boldsymbol{\epsilon}$ is the polarization vector of the photon, and $\boldsymbol{\alpha}$ is the vector of Dirac α matrices. The amplitude $\mathcal{M}_{fi}$ was considered in detail in the literature [12–14] as well as in our previous studies [15,16] and need not be discussed further.

The angle-differential cross section of the process is connected to the amplitude by

$$\frac{d\sigma}{d\Omega} = |\mathcal{M}_{fi}|^2 . \tag{3}$$

It depends on the polarization vectors of the initial and the scattered photons. In order to obtain the angle-differential cross section observed in an experiment, the above expression should be averaged over the polarization distribution of the incident radiation and, if the final polarization is not detected, summed over the polarizations of the scattered radiation.

In the present work, we are interested in the scattering off the closed-shell atoms, for which $J_i = M_i = J_f = M_f = 0$. In this case, due to symmetry considerations, the transition amplitude can be parameterized [5] by the parallel $\mathcal{A}_{||}$ and perpendicular $\mathcal{A}_{\perp}$ amplitudes,

$$\mathcal{M}_{fi} = \boldsymbol{\epsilon}_{i||} \cdot \boldsymbol{\epsilon}^*_{f||} \, \mathcal{A}_{||} + \boldsymbol{\epsilon}_{i\perp} \cdot \boldsymbol{\epsilon}^*_{f\perp} \, \mathcal{A}_{\perp} , \tag{4}$$

where $\boldsymbol{\epsilon}_{||}$ and $\boldsymbol{\epsilon}_{\perp}$ are the components of the polarization vector parallel and perpendicular to the scattering plane (i.e., the plane spanned by vectors $\boldsymbol{k}_i$ and vectors $\boldsymbol{k}_f$). The amplitudes $\mathcal{A}_{||}$ and $\mathcal{A}_{\perp}$ depend only the photon energy ω and the scattering angle θ (i.e., the angle between $\boldsymbol{k}_i$ and $\boldsymbol{k}_f$).

We can use Eq. (4) to express all observable quantities in terms of amplitudes $\mathcal{A}_{||}$ and $\mathcal{A}_{\perp}$. In particular, the *unpolarized* angle-differential cross section (averaged over the initial-photon polarizations and summed over the final-photon polarizations) is just

$$\frac{d\sigma^{\rm unpol}}{d\Omega} = \frac{1}{2}(|\mathcal{A}_{||}|^2 + |\mathcal{A}_{\perp}|^2). \tag{5}$$

For the linearly polarized incident radiation, the angle-differential cross section is [5]

$$\frac{d\sigma^{\rm lin}}{d\Omega} = \frac{1}{4}(1 + \xi_{1i}\,\xi_{1f})(|\mathcal{A}_{||}|^2 + |\mathcal{A}_{\perp}|^2) + \frac{1}{4}(\xi_{1i} + \xi_{1f})\,(|\mathcal{A}_{||}|^2 - |\mathcal{A}_{\perp}|^2) , \tag{6}$$

where $\xi_1 = \epsilon_{||}^2 - \epsilon_{\perp}^2$. In the particular case when the incident radiation is fully polarized and the polarization of the scattered radiation is not observed, the angle-differential cross section is defined only by the parallel amplitude,

$$\frac{d\sigma^{\rm lin}}{d\Omega} = |\mathcal{A}_{||}|^2. \tag{7}$$

In the present work, we are specifically interested in the Stokes parameter P_1 of the scattered radiation, which can be evaluated as

$$P_1 = \frac{d\sigma_{||}^{\rm lin}/d\Omega - d\sigma_{\perp}^{\rm lin}/d\Omega}{d\sigma_{||}^{\rm lin}/d\Omega + d\sigma_{\perp}^{\rm lin}/d\Omega} , \tag{8}$$

where $d\sigma_{||}^{\rm lin}/d\Omega$ and $d\sigma_{\perp}^{\rm lin}/d\Omega$ are the differential cross sections for the scattering of radiation polarized parallel to and perpendicular to the scattering plane, respectively. Using Eq. (6) and identifying the Stokes parameter P_1 of the incoming light as $P_{1i} = \xi_{1i}$, we obtain

$$P_{1f} = \frac{(1 + P_{1i})|\mathcal{A}_{||}|^2 - (1 - P_{1i})|\mathcal{A}_{\perp}|^2}{(1 + P_{1i})|\mathcal{A}_{||}|^2 + (1 - P_{1i})|\mathcal{A}_{\perp}|^2}. \tag{9}$$

This expression connects the degree of polarization of the incident and the scattered radiation. It shows, in particular, that the scattered radiation is always fully polarized ($P_{1f} = 1$) when the initial radiation is fully polarized ($P_{1i} = 1$).

III. CALCULATION OF AMPLITUDES

In this section, we discuss the calculation of the amplitudes $\mathcal{A}_{||}$ and $\mathcal{A}_{\perp}$, which are the main building blocks for all observable quantities.

Let us first define the geometry of the process. We chose the z axis of our Cartesian coordinate system along the momentum of the incoming photon $\boldsymbol{k}_i$ and the x axis along the polarization vector of the incoming photon $\boldsymbol{\epsilon}_i$. With this choice of the coordinate system, the angle-differential cross section depends on angles only through the polarization vector of the outgoing photon $\boldsymbol{\epsilon}_f$ and $\hat{\boldsymbol{k}}_f \equiv \boldsymbol{k}_f/|\boldsymbol{k}_f| = (\theta, \phi)$, where $\cos\theta = \hat{\boldsymbol{k}}_i \cdot \hat{\boldsymbol{k}}_f$. The plane spanned by vectors $\boldsymbol{k}_i$ and vectors $\boldsymbol{k}_f$ is commonly referred to as the scattering plane and the angle θ between them as the scattering angle.

Our calculations of the transition amplitudes of the Rayleigh scattering are performed within the independent particle approximation (IPA), in which the amplitudes of the scattering off individual electrons of the atomic target are taken to be additive. From these shell-dependent amplitudes, the total scattering amplitude is obtained as a sum

$$\mathcal{M}_{fi} = \sum_n \mathcal{M}_n = \sum_{njl} \mathcal{M}_{njl} , \tag{10}$$

where n, l, and j are the quantum numbers of the one-electron states and the summation runs over all occupied states. The individual contributions $\mathcal{M}_n$ with $n = 1, 2, 3$, etc., are referred to as the contributions of the K, L, M, ... shells. The IPA approximation is known to work fairly well, as discussed in Refs. [5,11,13]. This conclusion was also confirmed by numerical calculations of the electron-electron interaction corrections to Rayleigh scattering recently performed for helium-like ions in Ref. [17].

In the previous work [16], we described our approach to the calculation of the one-particle amplitudes $\mathcal{M}_{njl}$, which is based on a numerical solution of the Dirac equation for an electron in the central field of the nucleus and the "spectator" electrons. Specifically, we apply the power series expansion method for solving the radial Dirac equation with a general scalar potential $V(r)$ for an arbitrary energy E. Using the asymptotic form of the exact Dirac functions, we compute the regular and irregular solutions of the Dirac equation and store them on a radial grid. Knowing the regular and irregular Dirac solutions, we construct the Green's function of the Dirac equation, which is then used for computing the second-order matrix elements in Eq. (1). The numerical method is described in Ref. [18].

An important feature of the computation is a summation over the complete one-electron spectrum of the Dirac equation and, as a consequence, an infinite summation over the multipoles of the photon field L [which is referred to as the partial-wave (PW) expansion]. In our calculations, we extended the PW expansion up to $L_{\max} = 70$, which yielded converged results for the amplitudes of the K, L, M, and, sometimes, N shells in the expansion (10). For the higher n atomic shells, however, the convergence of the PW expansion becomes increasingly slower. Fortunately, numerical contributions of the shells with $n > 4$ decrease quickly, except for the forward scattering angles.

The contributions of the higher n shells can be accounted for within the so-called form-factor (FF) approximation, in which the photon scatters off a static charge distribution of individual electrons as obtained from the Dirac-Fock equation. Pratt and coworkers [13,14] reported a modified FF approximation that included some binding effects and estimates for the imaginary part of the amplitudes. Following Refs. [13,14], we define the approximate FF amplitudes by

$$\mathrm{Re}\,\mathcal{A}_{||,n} = -G_n(q)\cos\theta, \quad (11)$$

$$\mathrm{Re}\,\mathcal{A}_{\perp,n} = -G_n(q), \quad (12)$$

$$\mathrm{Im}\,\mathcal{A}_{||,n} = \left(\sigma_n^{\mathrm{PE}}/\sigma_{n_0}^{\mathrm{PE}}\right)\mathrm{Im}\,\mathcal{A}_{||,n_0}, \quad (13)$$

$$\mathrm{Im}\,\mathcal{A}_{\perp,n} = \left(\sigma_n^{\mathrm{PE}}/\sigma_{n_0}^{\mathrm{PE}}\right)\mathrm{Im}\,\mathcal{A}_{\perp,n_0}, \quad (14)$$

where $G_n(q)$ is the form factor of the n shell, σ_n^{PE} is the cross section for the photoionization from the nth shell, and n_0 is an inner shell for which partial-wave expansion results are available. The modified form factor is defined as [19]

$$G_n(q) = \int_0^\infty r^2 dr\, \rho_n(r)\,\frac{\sin qr}{qr}\,\frac{1}{\varepsilon_n - V_n(r)}, \quad (15)$$

where $q = 2\omega\sin(\theta/2)$ is the momentum transferred to the target atom by the scattered photon, ε_n is the energy of an electron in the nth shell (including the rest mass), $V_n(r)$ is the binding potential for electrons in the nth shell (including the nuclear Coulomb field and the screening potential from the other shells), and $\rho_n(r)$ is the electron charge density of the nth shell, normalized to the number of electrons in the shell, $\int_0^\infty r^2 dr\,\rho_n(r) = 2j_n + 1$.

In our numerical calculations, we use the partial-wave expansion (PWE) method to compute the amplitudes of the inner

TABLE I. Rayleigh-scattering amplitudes $\mathcal{A}_{||}$ and $\mathcal{A}_{\perp}$ for Pb ($Z = 82$) at photon energy $\omega = 145$ keV, in relativistic units. "PWE" labels results obtained within the partial-wave expansion; "FF" denotes results obtained within the modified form-factor approximation. n is the shell number ($n = 1$ is K shell, $n = 2$, L shell, etc.). The imaginary part of the FF amplitudes is scaled to match the corresponding PWE amplitude for the $n = 3$ shell, according to Eqs. (13) and (14).

		$\mathcal{A}_{\parallel}$(PWE)		$\mathcal{A}_{\parallel}$(FF)		$\mathcal{A}_{\perp}$(PWE)		$\mathcal{A}_{\perp}$(FF)	
θ (deg)	n	Re	Im	Re	Im	Re	Im	Re	Im
0	1	−1.9196	1.1357	−1.7238	1.0970	−1.9196	1.1357	−1.7238	1.0970
	2	−7.6961	0.2087	−7.6736	0.2047	−7.6961	0.2087	−7.6736	0.2047
	3	−17.7637	0.0480	−17.7633	0.0480	−17.7637	0.0480	−17.7633	0.0480
	4	−31.8873	0.0118	−31.8849	0.0122	−31.8873	0.0118	−31.8849	0.0122
	5			−17.9860	0.0025			−17.9860	0.0025
	6			−3.9995	0.0002			−3.9995	0.0002
30	1	−1.6287	0.9048	−1.4514	0.7763	−1.8748	1.1001	−1.6760	1.0242
	2	−4.7296	0.1494	−4.8036	0.1448	−5.5312	0.1956	−5.5467	0.1911
	3	−1.2674	0.0339	−1.3791	0.0339	−1.4904	0.0448	−1.5925	0.0448
	4	−0.5964	0.0084	−0.6185	0.0086	−0.6945	0.0110	−0.7142	0.0114
	5			−0.0867	0.0018			−0.1001	0.0023
	6			−0.0016	0.0001			−0.0019	0.0002
60	1	−0.8851	0.3701	−0.7775	0.1806	−1.7660	1.0142	−1.5550	0.8673
	2	−1.0626	0.0369	−1.2121	0.0337	−2.3606	0.1669	−2.4242	0.1618
	3	0.0110	0.0079	−0.0170	0.0079	−0.0249	0.0379	−0.0340	0.0379
	4	0.0261	0.0020	0.0206	0.0020	0.0406	0.0093	0.0411	0.0096
	5			0.0032	0.0004			0.0064	0.0020
	6			0.0001	0.0000			0.0001	0.0002
120	1	0.8031	−0.5380	0.6421	−0.4462	−1.5533	0.8397	−1.2843	0.6115
	2	0.1391	−0.0862	0.1440	−0.0832	−0.1876	0.1192	−0.2880	0.1141
	3	0.0696	−0.0195	0.0731	−0.0195	−0.1198	0.0267	−0.1462	0.0267
	4	0.0194	−0.0048	0.0205	−0.0050	−0.0341	0.0066	−0.0410	0.0068
	5			0.0041	−0.0010			−0.0081	0.0014
	6			0.0002	−0.0001			−0.0004	0.0001

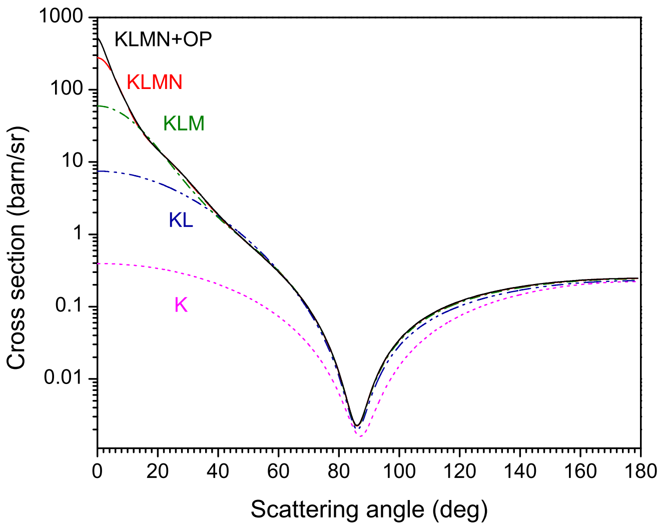

FIG. 1. Angle-differential cross section of the Rayleigh scattering of fully linearly polarized 145- keV x rays off the neutral lead atom (Pb, $Z = 82$). Solid line (black) shows results of the full calculation, with the PWE treatment of the $KLMN$ shells and the FF treatment of the OP shells. The other lines present results of the PWE calculations with inclusion of the $KLMN$ shells (dashed line, red), KLM shells (dash-dotted line, green), KL shells (dash-dot-dotted line, blue), and K shells (dotted line, magenta).

$n \leqslant n'$ shells (with $n' = 3$ or 4), and the modified FF approach to approximate the amplitudes for the remaining outer shells. This approach was previously used in calculations of Pratt and coworkers [13,14].

Table I compares results of the PWE calculation with those obtained in the modified FF approximation, for the case of scattering off neutral lead ($Z = 82$) and the photon energy of $\omega = 145$ keV. We observe that the FF approximation works very well for forward scattering angles. For larger angles and higher scattering energies, however, its accuracy gradually deteriorates. The use of the FF approximation is essential in order to obtain reliable results for the forward scattering, since the contribution of the outer $n > 4$ shells (for which no convergent PWE results are obtained) is significant in this case. For larger angles, however, the numerical contribution of the outer shells is small and can often be omitted.

Figure 1 displays the convergence of calculated results with respect to the number of shells taken into account, for the angle-differential cross section $d\sigma(\theta, \phi = 0)/d\Omega$ for the completely linearly polarized incident light with energy $\omega =$ 145 keV and neutral lead target. We observe that the contribution of shells with $n > 4$ is noticeable only in the very forward direction. We performed two variants of the full (PWE+FF) calculation, evaluating the contribution of the $n = 4$ shell by the PWE and FF methods. Both computations yielded results that are visually indistinguishable on the picture.

IV. DETERMINATION OF THE POLARIZATION PURITY OF THE INITIAL PHOTON

We now consider a correlation between the degree of linear polarization of the incoming and scattered x rays. Already

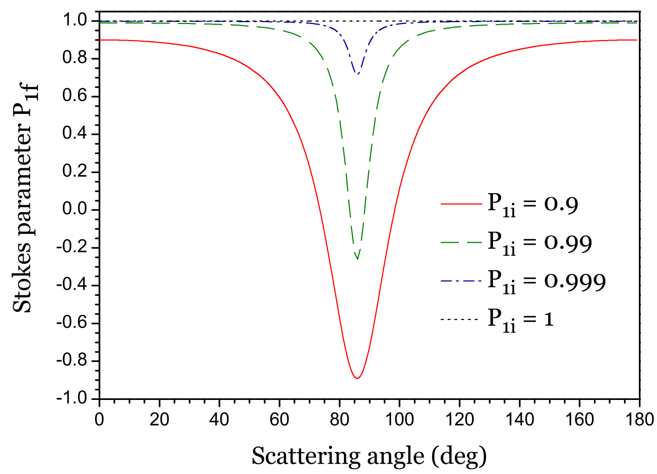

FIG. 2. The Stokes parameter of the scattered radiation P_{1f} as a function of the scattering angle θ, for different degrees of linear polarization of the incoming radiation P_{1i}, for scattering of the 145-keV x rays off the neutral lead atom (Pb, $Z = 82$).

from Eq. (4) it can be seen that if the incident radiation is polarized parallel or perpendicular to the scattering plane, the scattered radiation will have exactly the same polarization. A general relation between the Stokes parameters P_1 of the incident and scattered radiation is given by Eq. (9). Using the numerical results for the transition amplitudes obtained in the previous section, we can deduce results also for the Stokes parameters.

Figure 2 presents a typical example of the angular dependence of the Stokes parameter of the scattered radiation P_{1f} for different values of the Stokes parameter of the incident radiation P_{1i}. We observe that in the region of scattering angles $\theta \approx 90^\circ$ the degree of polarization of the scattered radiation depends strongly on the degree of polarization of the initial radiation. If, for example, the incident radiation is depolarized by just 0.1%, the depolarization of the scattered radiation might reach up to 20%.

From Fig. 1, we conclude that the vicinity of scattering angles $\theta \approx 90^\circ$ is the region of the suppressed photon emission and, according to Eq. (7), of small values of the parallel amplitude $A_{||}$. (We recall that in the form-factor approximation, $A_{||} \propto \cos^2\theta$). For the angles $\theta \approx 90^\circ$ and the incident radiation of high polarization purity ($1 - P_{1i} \ll 1$), the numerator and the denominator of Eq. (9) are composed of two small quantities, $(1 + P_{1i})|A_{||}|^2$ and $(1 - P_{1i})|A_\perp|^2$, so that even small variations of the amplitudes and the initial polarization may lead to large changes of the polarization of the scattered radiation.

This effect can be used as a method for an accurate determination of small depolarization of initial photon $\delta_i \equiv 1 - P_{1i}$, by measuring the Stokes parameter of the scattered radiation P_{1f} at scattering angles θ around 90°. We note that despite the strong suppression of the cross section at $\theta \approx 90^\circ$, this angle region is still accessible for experimental investigations [6], due to great luminosity of synhrotron radiation on modern facilities.

This remarkable effect can be understood more easily if we rewrite Eq. (9) in terms of the depolarization of the initial

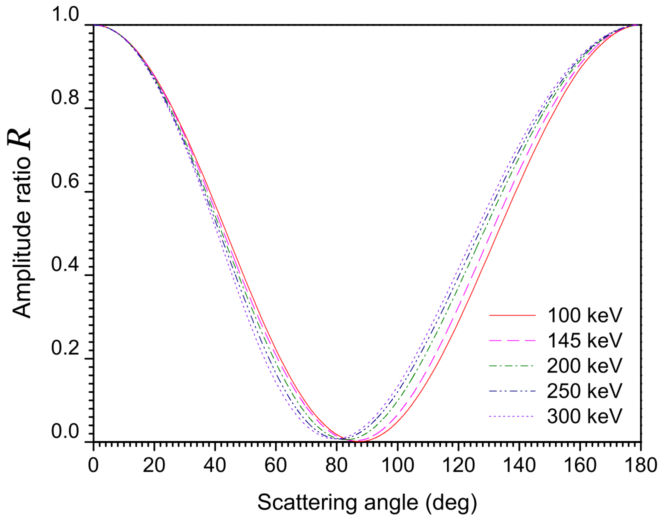

FIG. 3. The ratio of the squares of the parallel and perpendicular amplitudes $R(E,\theta)$ as a function of the scattering angle θ, for scattering of the x rays off neutral lead atom (Pb, $Z = 82$).

radiation δ_i as

$$P_{1f} = 1 - \frac{2}{1 + \frac{2-\delta_i}{\delta_i} R(E,\theta)}, \tag{16}$$

where R is the ratio of the squares of the parallel and perpendicular amplitudes,

$$R(E,\theta) = \frac{|A_{||}|^2}{|A_{\perp}|^2}. \tag{17}$$

We note that within the (standard) form-factor approximation, $R(E,\theta)$ does not depend on energy and is just $R(E,\theta) = R_{\rm FF}(\theta) = \cos^2\theta$, so that Eq. (16) becomes an universal function, without any dependence on the nuclear charge of the target or the energy of the incident radiation.

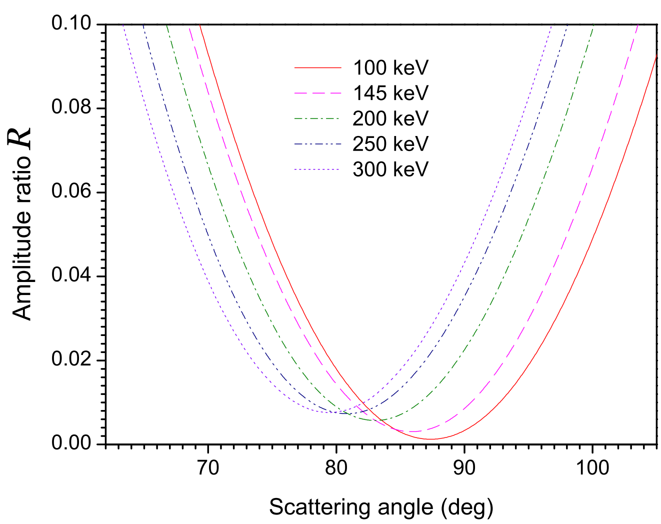

FIG. 4. A fragment of Fig. 3, for the angle region relevant for the determination of the polarization purity of the initial radiation.

In order to study the sensitivity of P_{1f} on δ_i, we differentiate Eq. (16), obtaining

$$\frac{\partial P_{1f}}{\partial \delta_i} = -\frac{4R(E,\theta)}{[R(E,\theta)(2-\delta_i)+\delta_i]^2}. \tag{18}$$

The derivative behaves as $-1/(2\delta_i)$ for $R \approx \delta_i/2 \ll 1$ and as $-1/R$ for $\delta_i \ll R \ll 1$. We conclude that by measuring the Stokes parameter of the outgoing radiation P_{1f} in the region of small values of $R(E,\theta)$, we achieve an enhanced sensitivity of our measurement to small depolarizations of the incoming radiation.

The angular dependence of the function $R(E,\theta)$ for different collision energies is plotted on Figs. 3 and 4, for scattering off the neutral lead target. The plotted results were obtained within the PWE approach with including shells with $n \leqslant 4$ for energies 100 and 145 keV and $n \leqslant 3$ for higher energies.

Contrary to the FF approximation, in which the function R vanishes at $\theta = 90^\circ$, the PWE calculation shows that the minimal value of R is always above zero. The minimal value

TABLE II. The ratio of the squares of the parallel and perpendicular amplitudes $R(E,\theta)$ for Rayleigh scattering off the neutral lead atom. "FF" denotes the (standard) form-factor approximation, with $R_{\rm FF}(\theta) = \cos^2\theta$.

θ (deg)	E (keV)	R
30	FF	0.7500
	100	0.7394 (3)
	145	0.7335 (3)
	200	0.7224 (4)
	250	0.7148 (10)
	300	0.7095 (15)
60	FF	0.2500
	100	0.2212 (4)
	145	0.2077 (6)
	200	0.1888 (7)
	250	0.1646 (9)
	300	0.1425 (15)
70	FF	0.1170
	100	0.0926 (4)
	145	0.0837 (4)
	200	0.0663 (6)
	250	0.0497 (7)
	300	0.0386 (15)
80	FF	0.0302
	100	0.0176 (2)
	145	0.0143 (1)
	200	0.0088 (2)
	250	0.0074 (2)
	300	0.0077 (3)
90	FF	0.0000
	100	0.0030 (1)
	145	0.0085 (1)
	200	0.0225 (2)
	250	0.0352 (8)
	300	0.0436 (18)

gradually increases with the increase of the collision energy. The *position* of the minimum also shifts from the FF value $\theta = 90^\circ$ toward smaller angles; as the energy increases, the shift becomes larger. We observe that for a wide range of the collision energies, the angle region of $\theta = 60$–100° corresponds to values of $R \lesssim 0.1$, thus yielding an enhancement of sensitivity in determination of δ_i from one to two orders of magnitude.

The method of determining δ_i from Eq. (16) discussed so far depends on theoretical results for the function $R(E, \theta)$, which need to be obtained reliably and with a controlled accuracy. In Table II we present results of our calculations of $R(E, \theta)$ for the neutral lead target and different angles and scattering energies. In our calculation of $R(E, \theta)$, we found that the inclusion of the FF approximation for the higher n shells does not improve the convergence of the calculated results for the scattering angles we are presently interested, so we did not include it. The uncertainty ascribed to the numerical values of $R(E, \theta)$ reflects our estimation of the error caused by an incomplete treatment of the outer electron shells.

We neglect uncertainty due to smaller effects not included into calculation, even though they might be enhanced in the region of $\theta \approx 90^\circ$. Among these effects, the largest one is probably the residual electron correlation, studied (to first order in $1/Z$ and for He-like ions) in Ref. [17]. The results of Ref. [17] suggest that an enhancement around 90° exists but the change of the cross section is still very small.

One can avoid the need of theoretical predictions for $R(E, \theta)$ by measuring an independent observable that depends on δ_i and $R(E, \theta)$. We propose to use for this purpose the ratio of the angle-differential cross sections measured *within* and *perpendicular* to the plane of polarization of the incident radiation. This ratio can be evaluated as

$$\sigma_R \equiv \frac{d\sigma(\boldsymbol{\epsilon}_{i\|})/(d\Omega)}{d\sigma(\boldsymbol{\epsilon}_{i\perp})/(d\Omega)} = \frac{1 + \frac{2-\delta_i}{\delta_i} R(E, \theta)}{R(E, \theta) + \frac{2-\delta_i}{\delta_i}}, \tag{19}$$

where we assumed that the polarization of the scattered photons remains unobserved.

Therefore, by measuring P_{1f} and σ_R for the same scattering energy E and scattering angle θ, we can determine the degree of polarization of the initial radiation δ_i from Eqs. (16) and (19), without any further theoretical input.

V. CONCLUSION

We have studied the polarization properties of x-ray radiation elastically scattered off a closed-shell atomic target. We have shown, in particular, that the degree of polarization of the scattered radiation is very sensitive to small deviations of the incident radiation from the 100% linear polarization, especially in the region of scattering angles $\theta = 80$–90°. This effect can be used as a precision tool for the diagnostics of the polarization purity of the synchrotron radiation. Two variants of the diagnostics method have been put forward. The first one requires the ratio of the squared amplitudes $R(\theta, E)$ to be taken from theoretical calculations, whereas the second one determines $R(\theta, E)$ from an additional measurement of the ratio of the scattering cross section observed within and perpendicular to the polarization plane of the incident radiation.

ACKNOWLEDGMENTS

V.A.Y. and A.V. acknowledge support by the Russian Foundation for Basic Research Grant No. 16-02-00538-a. V.A.Y. acknowledges also support from the Ministry of Education and Science of the Russian Federation Grants No. 3.5397.2017/6.7 and No. 3.1463.2017/4.6.

[1] S. Tashenov, T. Bäck, R. Barday, B. Cederwall, J. Enders, A. Khaplanov, Y. Poltoratska, K.-U. Schässburger, and A. Surzhykov, Phys. Rev. Lett. **107**, 173201 (2011).

[2] R. Märtin, G. Weber, R. Barday, Y. Fritzsche, U. Spillmann, W. Chen, R. D. DuBois, J. Enders, M. Hegewald, S. Hess, A. Surzhykov, D. B. Thorn, S. Trotsenko, M. Wagner, D. F. A. Winters, V. A. Yerokhin, and Th. Stöhlker, Phys. Rev. Lett. **108**, 264801 (2012).

[3] S. Tashenov, T. Bäck, R. Barday, B. Cederwall, J. Enders, A. Khaplanov, Y. Fritzsche, K.-U. Schässburger, A. Surzhykov, V. A. Yerokhin, and D. Jakubassa-Amundsen, Phys. Rev. A **87**, 022707 (2013).

[4] O. Kovtun, V. Tioukine, A. Surzhykov, V. A. Yerokhin, B. Cederwall, and S. Tashenov, Phys. Rev. A **92**, 062707 (2015).

[5] S. C. Roy, B. Sarkar, L. D. Kissel, and R. H. Pratt, Phys. Rev. A **34**, 1178 (1986).

[6] K.-H. Blumenhagen, S. Fritzsche, T. Gassner, A. Gumberidze, R. Märtin, N. Schell, D. Seipt, U. Spillmann, A. Surzhykov, S. Trotsenko, G. Weber, V. A. Yerokhin, and T. Stöhlker, New J. Phys. **18**, 103034 (2016).

[7] J. Stöhr, H. A. Padmore, S. Anders, T. Stammler, and M. R. Scheinfein, Surf. Rev. Lett. **5**, 1297 (1998).

[8] M. Ghidini, F. Maccherozzi, X. Moya, L. C. Phillips, W. Yan, J. Soussi, N. Métallier, M. E. Vickers, N.-J. Steinke, R. Mansell *et al.*, Adv. Mater. **27**, 1460 (2015).

[9] H. A. Dürr, E. Dudzik, S. S. Dhesi, J. B. Goedkoop, G. van der Laan, M. Belakhovsky, C. Mocuta, A. Marty, and Y. Samson, Science **284**, 2166 (1999).

[10] J. Arthur, Nuovo Cimento **18D**, 213 (1996).

[11] S. C. Roy, L. Kissel, and R. H. Pratt, Radiat. Phys. Chem. **56**, 3 (1999).

[12] W. R. Johnson and K.-T. Cheng, Phys. Rev. A **13**, 692 (1976).

[13] L. Kissel, R. H. Pratt, and S. C. Roy, Phys. Rev. A **22**, 1970 (1980).

[14] P. Kane, L. Kissel, R. Pratt, and S. Roy, Phys. Rep. **140**, 75 (1986).

[15] A. Surzhykov, V. A. Yerokhin, T. Jahrsetz, P. Amaro, T. Stöhlker, and S. Fritzsche, Phys. Rev. A **88**, 062515 (2013).

[16] A. Surzhykov, V. A. Yerokhin, T. Stöhlker, and S. Fritzsche, J. Phys. B **48**, 144015 (2015).

[17] A. V. Volotka, V. A. Yerokhin, A. Surzhykov, T. Stöhlker, and S. Fritzsche, Phys. Rev. A **93**, 023418 (2016).

[18] V. A. Yerokhin, Phys. Rev. A **83**, 012507 (2011).

[19] W. Franz, Z. Phys. **98**, 314 (1936).